Title

A canonical approach to multi-dimensional van der Waals, hydrogen-bonded, and halogen-bonded potentials

Authors

Walton, Jay R
Rivera-Rivera, Luis A
Lucchese, Robert R
et al.

Publication Date

2016-05-01

DOI

10.1016/j.chemphys.2016.01.011

Peer reviewed

A Canonical Approach to Multi-dimensional van der Waals, Hydrogen-Bonded, and Halogen-Bonded Potentials

Jay R. Walton

Department of Mathematics, Texas A&M University, College Station, Texas 77843-3368

Luis A. Rivera-Rivera, Robert R. Lucchese, and John W. Bevan*

Department of Chemistry, Texas A&M University, College Station, Texas 77843-3255

Abstract

A canonical approach is used to investigate prototypical multi-dimensional intermolecular interaction potentials characteristic of categories in van der Waals, hydrogen-bonded, and halogen-bonded intermolecular potential energy functions. It is demonstrated that well-characterized potentials in Ar•HI, OC•HI, OC•HF, and OC•BrCl, can be canonically transformed to a common dimensionless potential with relative error less than 0.010. The results indicate common intrinsic bonding properties despite other varied characteristics in the systems investigated. The results of these studies are discussed in the context of the previous statement made by J. C. Slater [J. Chem. Phys. 57 (1972) 2389] concerning fundamental bonding properties in the categories of interatomic interactions analyzed.

* To whom correspondence should be addressed. E-mail: bevan@mail.chem.tamu.edu

1. Introduction

In 1972, J. C. Slater made a thought provoking statement [1]: *there is no very fundamental distinction between the van der Waals binding and covalent binding.* This has subsequently been the subject of extensive discussion [2]. To give a different perspective on this statement, we recently introduced formulations for the concept of canonical transformations [3] in the potentials of both diatomic and two body intermolecular interactions with no adjustable parameters [4]. The term canonical potential for a class of interatomic molecular systems refers to a dimensionless function obtained from each molecule within the defined class by a readily invertible algebraic transformation. Furthermore, to be deemed canonical, the dimensionless potentials obtained from all of the molecules by the canonical transformation within the defined class must agree to within a specified order of accuracy. Different classes of representative ground electronic state pairwise interatomic interactions were referenced to a chosen canonical potential illustrating application of such transformations. Accurately determined potentials of the diatomic molecules H_2, H_2^+, HF, LiH, argon dimer, and one-dimensional dissociative coordinates in intermolecular Ar-HBr, OC-HF, and OC-Cl_2 were investigated throughout their ground state bound potentials. The results indicated that an explicit transformation developed specifically for the Born-Oppenheimer potential [5] of H_2 [6] could be applied to the other selected two body molecular potentials used to generate such a corresponding canonical potential. These applications included interatomic interactions that initially had been only partially corrected for non-Born-Oppenheimer effects [7-10]. We then studied a generalized formulation of canonical transformations [4] and spectra, and used it to investigate the concept of a canonical potential strictly within the Born-Oppenheimer approximation [11]. However, until very recently when a proof-of-concept analysis of the van der Waals dimer Ar•HBr was investigated [12],

corresponding canonical transformations have not been investigated for polyatomic systems which involve higher vibrational dimensions.

In this work, we now extend this type of canonical application to higher dimensional systems [12]. Reported results for canonical transformations in a range of different categories of intermolecular interactions including Ar•HI, OC•HI, OC•HF, and OC•BrCl, will be considered to demonstrate wider application of the proof-of-concept analysis of Ar•HBr. Specifically, investigation of these prototypes are demonstrated to canonically transform to a common dimensionless potential to high accuracy and then these intermolecular interactions will again be considered from the perspective of the statement made by Slater [1].

2. Method

The methodology used in the present study is an extension of the previous proof-of-concept investigation of Ar•HBr [12]. In the current investigation, the reference potential is again selected to be that for H_2^+, the simplest molecule [13]. In brief review, for the potential $E(R)$ with associated force distribution $F\left(R\right)=-E'\left(R\right)$, we define R_e and R_m to be the equilibrium nuclear separation, that is, the internuclear distance for which $F(R_e) = 0$, and the nuclear separation distance of maximum attractive force, that is $F(R_m)=-F_m$, respectively. We note that $R_e < R_m$. We also defined R_j^a and R_j^r by: $F(R_j^a)=-F_m / 2^j$ and $F\left(R_j^r\right)=F_m 2^j$.

The multi-dimensional potentials of Ar•HI, OC•HI, OC•HF, and OC•BrCl can be approximated using similar procedures introduced in Ref. 12. Specifically, one takes a sequence of angles $\theta_{1,\ldots,}\theta_{k,}$ and represent each of the radial potentials $E(\theta_k,R)$ using a selection of dyadic radial values $R_j^a(\theta_k)$ and corresponding values on the repulsive side. Piecewise affine

transformations are then applied to portions of the reference canonical radial potential (H_2^+) onto corresponding portions of the 1-D radial potentials $E(\theta_k,R)$ for each angle θ_k. For illustrative purposes in this work, for each θ_k, R_e and eight additional R-values, four on the attractive side and four corresponding values on the repulsive side, were selected for use in the construction. Spline interpolation is then used to approximate $E(\theta,R)$ for all other angular values θ. On the attractive side, the R values used are: $R_e < R_1^a(\gamma_1^a) < R_2^a(\gamma_2^a) < R_3^a(\gamma_3^a) < R_4^a(\gamma_4^a)$. The γ_j^a values are calculated so that affine canonical transformation for both the reference and target molecules interpolates the midpoint as well as the endpoints of the appropriate interval. In particular, the reference canonical form considered in the interval $R_e^* < R < R_1^{*a}$

$$\bar{E}_1^a(x) = \frac{E^*(xR_1^{*a} + (1-x)R_e^*) - E^*(R_e^*)}{E^*(R_1^{*a}) - E^*(R_e^*)} \tag{1}$$

and the corresponding canonical forms for the target molecules for a given value of θ_k

$$\tilde{E}_1^a(x;\gamma_1^a) = \frac{E(xR_1^a(\gamma_1^a) + (1-x)R_e) - E(R_e)}{E(R_1^a(\gamma_1^a)) - E(R_e)} \tag{2}$$

for $R_e < R < R_1^a(\gamma_1^a)$. The parameter γ_1^a is then chosen so that Eqs. (1) and (2) agree when x = 0.5. It is noticed that by construction, Eqs. (1) and (2) agree for x = 0 and 1. Inductively, for $R_1^{*a} < R < R_2^{*a}$ the reference canonical form is defined as

$$\bar{E}_2^a(x) = \frac{E^*(xR_2^{*a} + (1-x)R_1^{*a}) - E^*(R_1^{*a})}{E^*(R_2^{*a}) - E^*(R_1^{*a})} \tag{3}$$

and for $R_1^a(\gamma_1^a) < R < R_2^a(\gamma_2^a)$ the corresponding canonical forms for the target molecules for a given value of θ_k are defined as

$$\tilde{E}_2^{\mathrm{a}}(x;\gamma_2^{\mathrm{a}}) = \frac{E(xR_2^{\mathrm{a}}(\gamma_2^{\mathrm{a}}) + (1-x)R_1^{\mathrm{a}}(\gamma_1^{\mathrm{a}})) - E(R_1^{\mathrm{a}}(\gamma_1^{\mathrm{a}}))}{E(R_2^{\mathrm{a}}(\gamma_2^{\mathrm{a}})) - E(R_1^{\mathrm{a}}(\gamma_1^{\mathrm{a}}))}. \tag{4}$$

γ_2^{a} is selected so that Eqs. (3) and (4) agree for $x = 0.5$. Similar constructions apply for $j = 3$ and 4 on the attractive side and then on the repulsive side. The inverse canonical transformations are now employed to construct an approximation to the potential for the target molecules from the reference potential. More specifically, the inverse canonical transformations are considered corresponding to Eqs. (1) and (2):

$$E^*(R) = E^*(R_{\mathrm{e}}^*) + (E^*(R_1^{*\mathrm{a}}) - E^*(R_{\mathrm{e}}^*))\bar{E}_{\mathrm{e1}}^{\mathrm{a}}(x) \tag{5}$$

$$E(R) = E(R_{\mathrm{e}}) + (E(R_1^{\mathrm{a}}(\gamma_1^{\mathrm{a}})) - E(R_{\mathrm{e}}))\tilde{E}_{\mathrm{e1}}^{\mathrm{a}}(x;\gamma_1^{\mathrm{a}}). \tag{6}$$

The key to the construction is to replace Eq. (2) in Eq. (6) by Eq. (1) but with $x = (R - R_{\mathrm{e}})/(R_1^{\mathrm{a}}(\gamma_1^{\mathrm{a}}) - R_{\mathrm{e}})$ giving

$$E(R) = E(R_{\mathrm{e}}) + (E(R_1^{\mathrm{a}}(\gamma_1^{\mathrm{a}})) - E(R_{\mathrm{e}}))\frac{E^*(xR_1^{*\mathrm{a}} + (1-x)R_{\mathrm{e}}^{*\mathrm{a}}) - E^*(R_{\mathrm{e}}^{*\mathrm{a}})}{E^*(R_1^{*\mathrm{a}}) - E^*(R_{\mathrm{e}}^{*\mathrm{a}})}. \tag{7}$$

Similar constructions apply to $R_1^{\mathrm{a}}(\gamma_1^{\mathrm{a}}) < R < R_2^{\mathrm{a}}(\gamma_2^{\mathrm{a}})$, $R_2^{\mathrm{a}}(\gamma_2^{\mathrm{a}}) < R < R_3^{\mathrm{a}}(\gamma_3^{\mathrm{a}})$, and $R_3^{\mathrm{a}}(\gamma_3^{\mathrm{a}}) < R < R_4^{\mathrm{a}}(\gamma_4^{\mathrm{a}})$, as well as those on the repulsive side.

3. Results and Discussion

Morphed potentials have been previously determined for the systems OC•HI (4-D), OC•HF (6-D), and OC•BrCl (5-D) [14-16] from available spectroscopic data. Effective 2-D potentials for the dimers were calculated by fixing the OC molecule at a linear configuration and varying the center of mass separation and the angle of the second diatomic, while keeping the complex in a planar configuration. In OC•HI the bond length of the monomers were fixed to

1.128323 and 1.60916 Å, respectively, for CO and HI. In OC•HF, the bond length of both monomers were adiabatically average in their vibrational ground sate. In OC•BrCl, the BrCl bond length was fixed to 2.1361 Å and the CO bond length was adiabatically averaged in its vibrational ground sate.

We have regenerated the 2-D morphed potential of Ar•HI (HI bond length fixed to 1.60916 Å) in order to increase its accuracy [17]. The currently generated morphed potential is now based on a new MP2/aug-cc-pVQZ potential, where the basis set for iodine was chosen to be aug-cc-pVQZ-PP. These changes were made in the morphed potential of Ar•HI in order to extend the radial potential to 2.5 Å on the repulsive side and to 8.0 Å on the attractive side of the potential. The old and the new morphed potentials were found to be of similar quality.

Figure 1 shows different radial cuts at 10° intervals through the potentials of Ar•HI, OC•HI, OC•HF, and OC•BrCl. $\theta = 0°$ corresponds to the linear isomer Ar-HI, OC-HI, OC-HF, and OC-BrCl. $\theta = 180°$ corresponds to the linear isomer Ar-IH, OC-IH, OC-FH, and OC-ClBr. It is noted that the OC-HF complex is not bound for $\theta > 80°$. The latter upper limitation of the current canonical approach is due to requirements of bound states in the analysis. The central portion of Fig. 1 shows the canonical potential for all radial potentials of Ar•HI, OC•HI, OC•HF, and OC•BrCl characterized in real phase space. This figure demonstrates that the canonical nature of the radial potentials in these systems are independent of the angular degree of freedom as they are transformed to the same canonical curve.

On the left side Fig. 2 shows a subset of the radial cuts of the potentials of Ar•HI, OC•HI, OC•HF, and OC•BrCl selected at $\theta = 10°$, 90°, and 170°. The right side of the figure illustrates the canonical radial potentials with the addition of the H_2^+ (solid black lines) canonical potential for comparison. This demonstrates that to high accuracy, the radials potentials of Ar•HI, OC•HI,

OC•HF, OC•BrCl, and H_2^+ are canonical and furthermore suggests that the radial canonical potential of the simplest molecule H_2^+ [13] can be used to generate the multi-dimensional potentials of Ar•HI, OC•HI, OC•HF, and OC•BrCl provided there is sufficient independent data available for that potential from another independent source whether generated by experiment or alternative computational methods.

In Figs. 3 to 6, we present the 2-D cut of the potential energy surface and the relative error of Ar•HI and OC•BrCl generated by using the H_2^+ canonical potential as a reference molecule. The relative errors in the surfaces are approximately less than the very small value of 0.010 over the whole surface for all systems considered here. It is noted that the corresponding relative error for Ar•HBr is 0.0008, significantly better than the systems considered here. This is attributed to the superior characterization of the morphed potential in Ar•HBr as determined by the greater range of spectroscopic information needed to characterized the morphed potential. In addition, this canonical transformation is only completely applicable where there is an attractive force in the radial direction, which occurs in all the systems we have considered except for OC-HF complex for $\theta > 80°$.

From the previously published canonical treatment of Ar•HBr [12], we demonstrated that the 1-D canonical transformation with respect to the radial degree of freedom is independent of the angular degree of freedom of the potential energy surface. Furthermore, we showed that this multi-dimensional potential which is usually categorized as a van der Waals interaction, could be correlated with the corresponding 1-D canonical potential of the simplest molecule, the one electron diatomic H_2^+. Consequently, the potential energy surface of this intermolecular interaction can be accurately generated from the 1-D canonical ground state potential of H_2^+ together with independent additional data relevant to the polyatomic such as that supplied by

experiment or reliable quantum mechanical calculation. This indicated that the proposed canonical approach could have widespread potential applications in characterization of potential energy surfaces of molecular systems with vibrationally higher dimensions both in intramolecular and intermolecular systems. In the current work, the canonical approach provides a basis for a unified perspective on bonding in the polyatomic intermolecular systems that has been the subject of investigation. Specifically, it is demonstrated that the radial potential in Ar•HBr [12], Ar•HI, OC•HI, OC•HF, and OC•BrCl are canonical independent of angular degree of freedom of the potential energy surface

4. Conclusions

In previous work [3,4], we demonstrated unification on the nature of bonding in pairwise interatomic interactions covering different bonding categories from van der Waals, halogen bonding, and hydrogen bonding to strongly bound covalent and ionic molecules. We have now demonstrated that multi-dimensional well-characterized potential energy functions in Ar•HBr [12], Ar•HI, OC•HI, OC•HF, and OC•BrCl can be canonically transformed to a common dimensionless potential that is indicative of commonality in the potential energy functions of these differing categories of intermolecular interactions. In certain respects these results can be regarded as an extension of J. C. Slater's thought provoking statement [1]: *there is no very fundamental distinction between the van der Waals binding and covalent binding*. However, in the case of the systems considered here, the statement is pertinent to different types of intermolecular interactions. In the case of the systems consider in this work, the emphasis is on a very fundamental distinction between differing categories of the broader and more generally

defined range of weakly bound van der Waals bonding that also includes hydrogen bonding, and halogen bonding.

Acknowledgments

We give special thanks to The Robert A Welch Foundation (Grant A747) for financial support in the form of postdoctoral fellowships for L.A. Rivera-Rivera. In addition, we thank LST/ST, the Laboratory for Molecular Simulation, the Supercomputing Facility, and the Institute for Applied Mathematics and Computational Science at Texas A&M University.

References

[1] J.C. Slater, J. Chem. Phys. 57 (1972) 2389.

[2] R.F.W. Bader, J. Hernández-Trujillo, F. Cortés-Guzmán, J. Comput. Chem. 28 (2007) 4.

[3] R.R. Lucchese, C.K. Rosales, L.A. Rivera-Rivera, B.A. McElmurry, J.W. Bevan, J.R. Walton, J. Phys. Chem. A 118 (2014) 6287.

[4] J.R. Walton, L.A. Rivera-Rivera, R.R. Lucchese, J.W. Bevan, Phys. Chem. Chem. Phys. 17, (2015) 14805.

[5] M. Born, R. Oppenheimer, Ann. Phys. 389 (1927) 457.

[6] K. Pachucki, Phys. Rev. A 82 (2010) 032509.

[7] R.N. Herman, A. Asgharian, J. Mol. Spectrosc. 19 (1966) 305.

[8] A.H.M. Ross, R.S. Eng, H. Kildal, Opt. Commun. 12 (1974) 433.

[9] J.K.G. Watson, Can. J. Chem. 82 (2004) 820.

[10] R.J. Le Roy, University of Waterloo Chemical Physics Research Report CP-657R, 2004.

[11] J.R. Walton, L.A. Rivera-Rivera, R.R. Lucchese, J.W. Bevan, J. Phys. Chem. A 119 (2015) 6753.

[12] J.R. Walton, L.A. Rivera-Rivera, R.R. Lucchese, J.W. Bevan, Chem. Phys. Lett. 639 (2015) 63.

[13] Private communication, D. W. Schwenke supplied the H_2^+ data.

[14] L.A. Rivera-Rivera, Z. Wang, B.A. McElmurry, F.F. Willaert, R.R. Lucchese, J.W. Bevan, R.D. Suenram, F.J. Lovas, J. Chem. Phys. 133 (2010) 184305.

[15] L.A. Rivera-Rivera, Z. Wang, B.A. McElmurry, R.R. Lucchese, J.W. Bevan, G. Kanschat, Chem. Phys. 390 (2011) 42.

[16] L.A. Rivera-Rivera, K.W. Scott, B.A. McElmurry, R.R. Lucchese, J.W. Bevan, Chem. Phys. 425 (2013) 162.

[17] B.A. McElmurry, R.R. Lucchese, J.W. Bevan, S.P. Belov, Phys. Chem. Chem. Phys. 6 (2004) 5318.

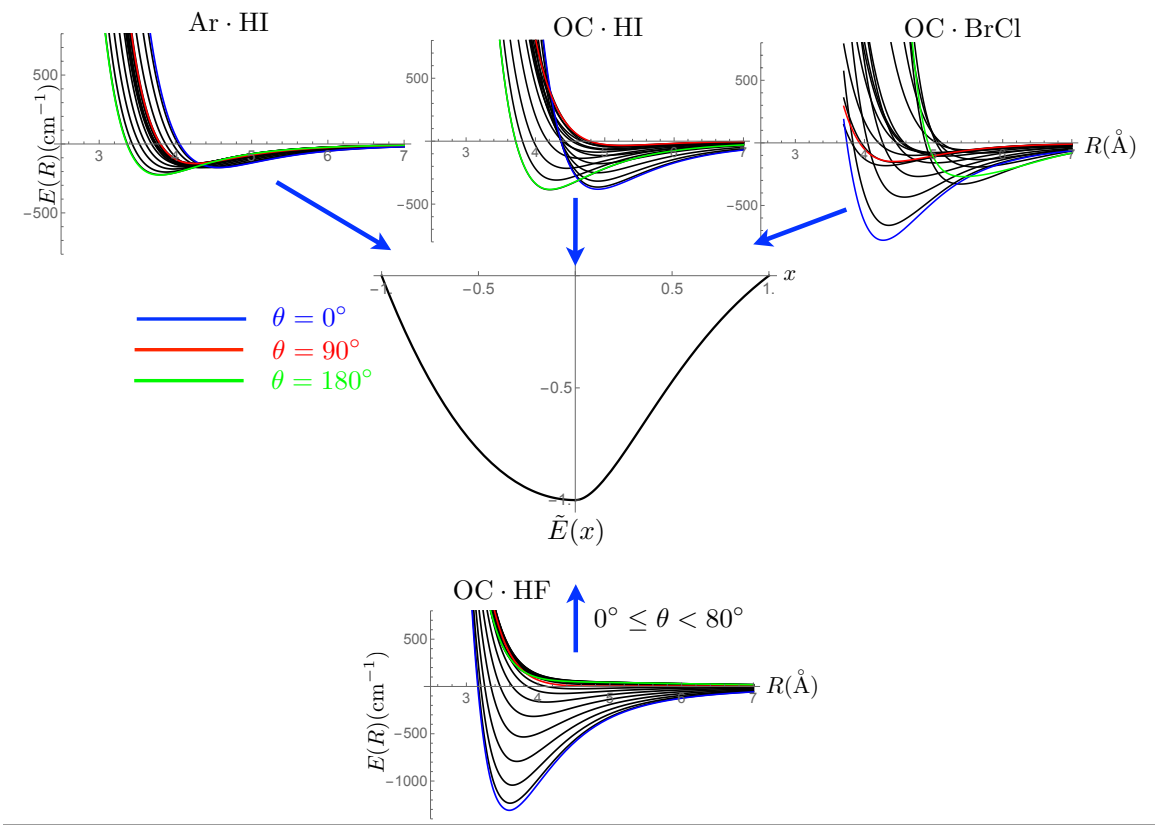

Figure 1. Radial cuts of the potentials of Ar•HI, OC•HI, OC•HF, and OC•BrCl at different values of θ from 0° to 180° every 10°. The central portion of the figure shows the canonical potential for all radial potentials of Ar•HI, OC•HI, OC•HF, and OC•BrCl. On the repulsive side the canonical potential is evaluated at -x, $-1 \leq x \leq 0$. Note that the OC•HF complex is not bound for $\theta > 80°$.

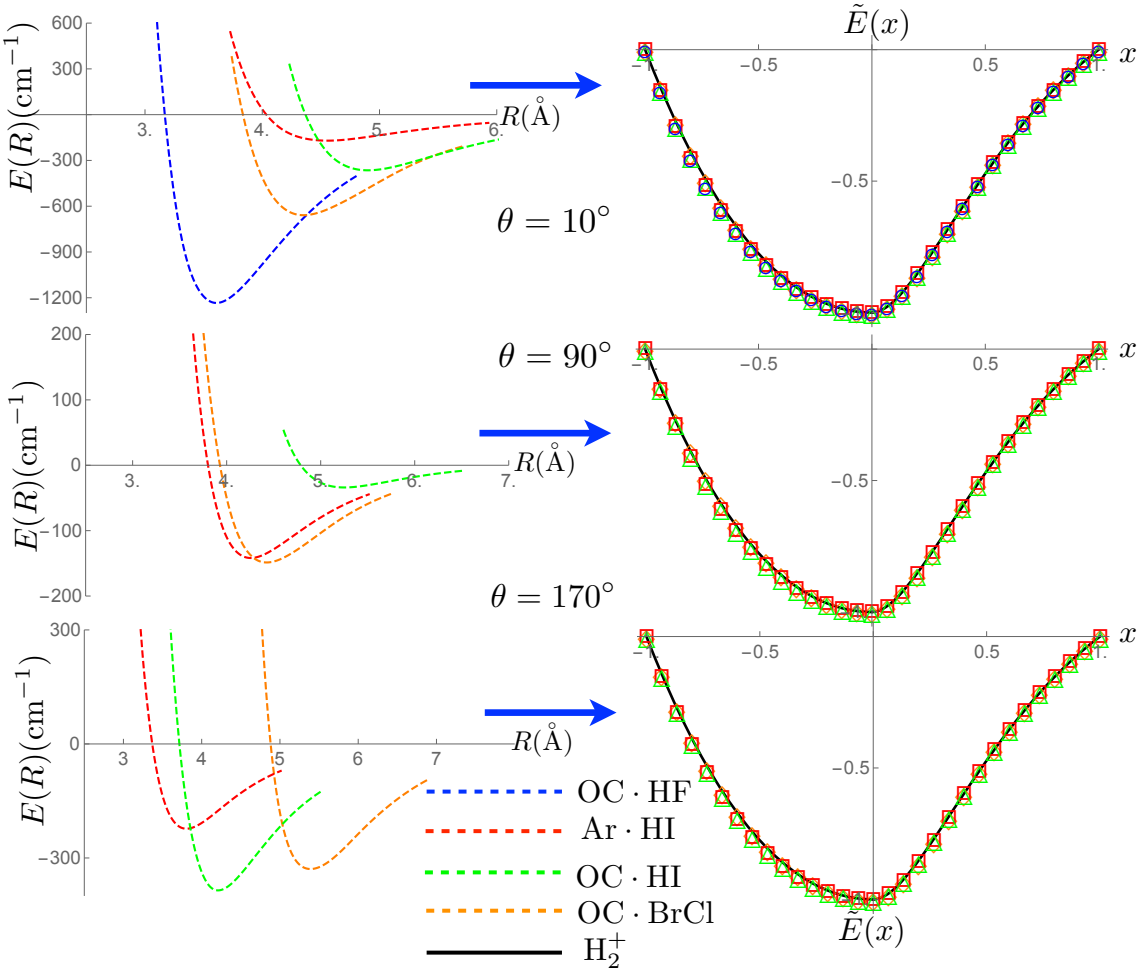

Figure 2. The left side of the figure shows the radial cuts of the potentials of Ar•HI, OC•HI, OC•HF, and OC•BrCl at θ = 10°, 90°, and 170°. Note that the OC•HF complex is not bound for θ > 80°. The right side of the figure shows the canonical radial potentials with the addition of the H_2^+ (solid black lines) canonical potential. On the repulsive side the canonical potential is evaluated at -x, -1 ≤ x ≤ 0.

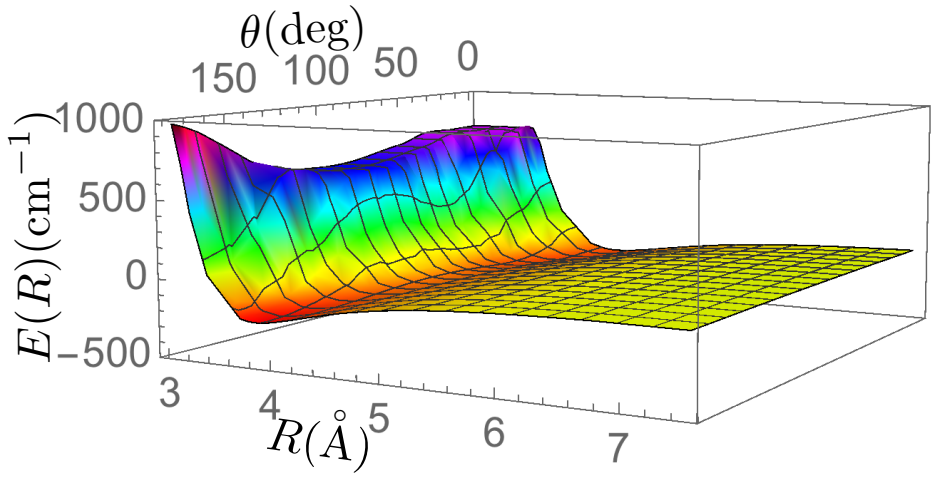

Figure 3. Generated adiabatic potential energy surface of Ar•HI, constructed from the 1-D potential curve for H_2^+.

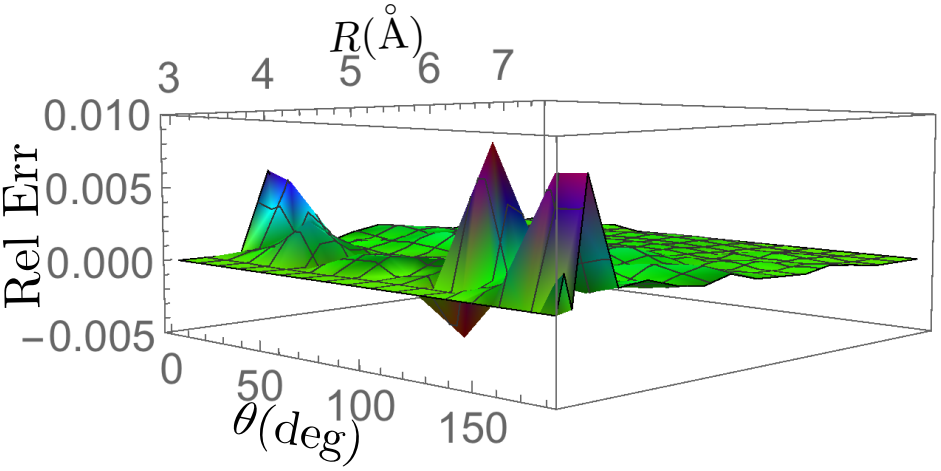

Figure 4. Pointwise relative error on the estimated potential energy surface of Ar•HI shown in Fig. 3, compared to the morphed potential of Ar•HI.

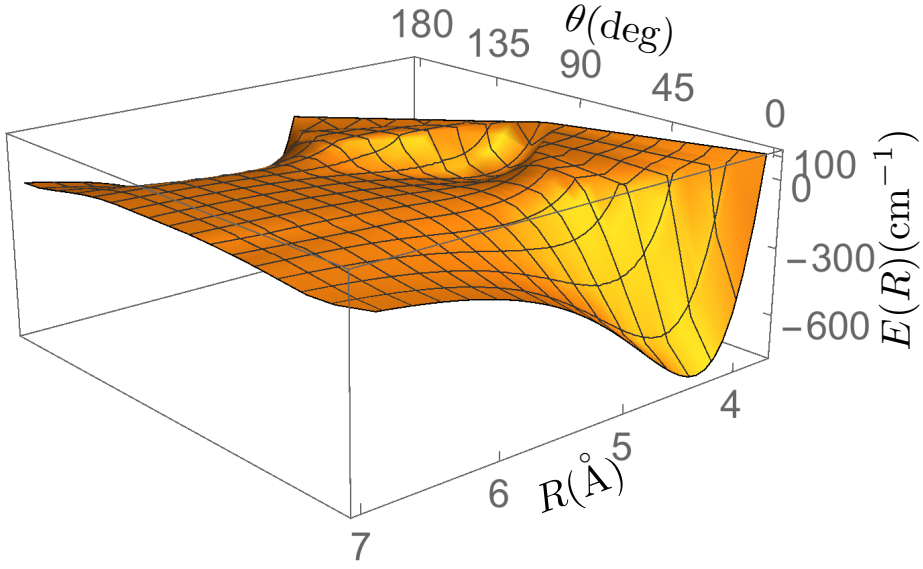

Figure 5. Generated adiabatic potential energy surface of OC•BrCl, constructed from the 1-D potential curve for H_2^+.

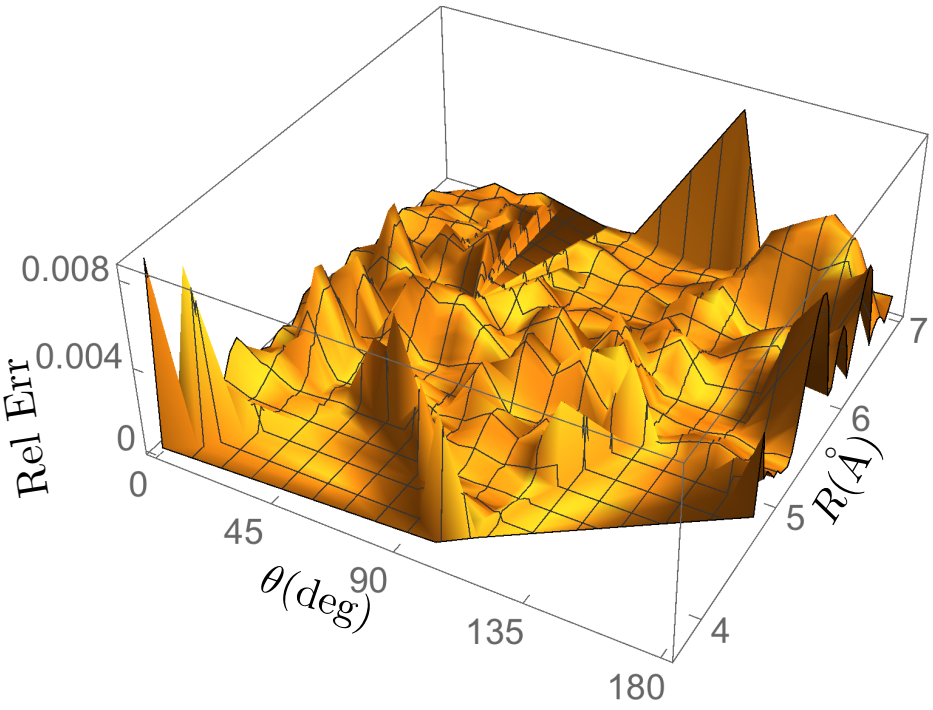

Figure 6. Pointwise relative error on the estimated potential energy surface of OC•BrCl shown in Fig. 5, compared to the morphed potential of OC•BrCl.